Inductive Micro Tri-Axial Tactile Sensor Using a CMOS Chip With a Coil Array

Sheng-Kai Yeh and Weileun Fang, *Fellow, IEEE*

***Abstract*— This letter presents a simple approach to implement the inductive-type micro tri-axial tactile sensor by integrating a complementary metal–oxide–semiconductor (CMOS) chip with sensing coils and a stainless steel sheet (as the sensing interface) using polymer encapsulation. In addition to the component integration, the polymer layer is exploited as the spring for the tactile sensor. The proposed CMOS-MEMS inductive tri-axial tactile sensor presents several features and advantages as follows: 1) the gap-closing inductive sensing approach is used for normal force (*Z*-axis) detection; 2) the area-change inductive sensing method is adopted for shear forces' (*X*-axis and *Y*-axis) detection; 3) the compact sensing coil array is implemented using the standard CMOS process; and 4) the polymer is employed as the encapsulation layer to cover and integrate the rigid stainless steel sheet sensing interface and the CMOS chip, while also acting as the spring to avoid the fragile suspended thin-film structure. To demonstrate the concept, a CMOS sensing chip with a 2 × 2 coil array is fabricated using the Taiwan Semiconductor Manufacturing Company standard process and is further integrated with a stainless steel sheet prepared by laser machining. The measurements indicate that the typical fabricated tri-axial inductive tactile sensor exhibits a normal load sensitivity (*Z*-axis) of 2.9 nH/N, an *X*-axis shear force sensitivity of 17.4 nH/N, and a *Y*-axis shear force sensitivity of 15.3 nH/N.**

***Index Terms*— Tri-axial tactile sensor, CMOS, inductive sensing.**

I. Introduction

TACTILE sensors could serve as important interfaces for human-machine or machine-machine interaction and hence have been applied in various fields such as robotics and consumer electronics. For example, the tri-axial tactile sensing devices are embedded on the surfaces of robot arms to help transduce the sensations of touch into electrical information [1]. Presently, most of the commercially available tri-axial load cells present size and cost concerns. To further extend the applications of a tri-axial tactile sensor, compact size and simple/low-cost processes are important design issues.

Micromachining processes have been extensively employed to implement micro tri-axial tactile sensors [2]–[15]. Presently, various chip-scale micro tactile sensors using the piezoresistive type [2]–[9] and capacitive type [10]–[15] sensing approaches have been successfully demonstrated. In general, special and complicated micromachining processes are required to fabricate these tactile sensors. Moreover, the deformation of suspended thin film structures is exploited as the sensing mechanism. Thus, the damage and process uniformity of fragile thin film structures become critical concerns during fabrication and operation. The polymer electromagnetic tri-axial tactile sensor was presented in [16]. As limited by the existing process, the sensor size is relatively large. A bulky tri-axial force sensor (on a printed circuit board) using eddy current was presented in [17]. A chip-scale inductive micro tactile sensor for a single axis (normal load detection only) was presented in [18]. However, damage to the sensing interface by shear force limits its applications and sensing range.

This letter leverages the standard CMOS process to design and fabricate the micro coil array on a sensing chip. The two-stage polymer molding processes are then employed to integrate and encapsulate the stainless steel sheet (as the sensing interface) and CMOS sensing chip. Thus, the tri-axial tactile sensor with no fragile suspended thin film structure can be realized using a simple fabrication process. Note that the future monolithic integration of sensing circuits on the CMOS chip can also be achieved. Measurements show that a typical tri-axial inductive tactile sensor (containing a 2.8 mm × 2.0 mm CMOS chip with a 2 × 2 sensing coil array) exhibits normal load sensitivity (Z-axis) of 2.9 nH/N, shear load sensitivity of 17.4 nH/N (X-axis), and 15.3 nH/N (Y-axis).

II. Design Principle

Fig. 1 shows the design and sensing scheme of the proposed inductive tri-axial tactile sensor. As shown in Fig. 1a-b, the sensor consists of a CMOS chip with a 2 × 2 sensing coil array along with a stainless steel sheet as the sensing interface. The CMOS chip and stainless steel sheet are integrated and encapsulated using the polymer. The polymer also acts as the spring for the proposed sensor, hence no fragile suspended thin film structure is required. Fig. 1c-d illustrate the sensing principle of the tri-axial inductive tactile sensor. As shown in Fig. 1c, the normal tactile load N_z (in the out-of-plane Z-axis)

Manuscript received February 1, 2019; revised February 18, 2019; accepted February 23, 2019. Date of publication February 27, 2019; date of current version April 2, 2019. This work was supported in part by GlobalMEMS Co. Ltd., Hsinchu, Taiwan, and in part by the Ministry of Science and Technology of Taiwan under Grant MOST 107-2218-E-007-022-. The review of this letter was arranged by Editor D. Shahrjerdi. *(Corresponding author: Weileun Fang.)*

The authors are with the Department of Power Mechanical Engineering, National Tsing Hua University, Hsinchu 30013, Taiwan, and also with the Institute of Nano Engineering and MicroSystems, National Tsing Hua University, Hsinchu 30013, Taiwan (e-mail: fang@pme.nthu.edu.tw).

Color versions of one or more of the figures in this letter are available online at http://ieeexplore.ieee.org.

Digital Object Identifier 10.1109/LED.2019.2901946

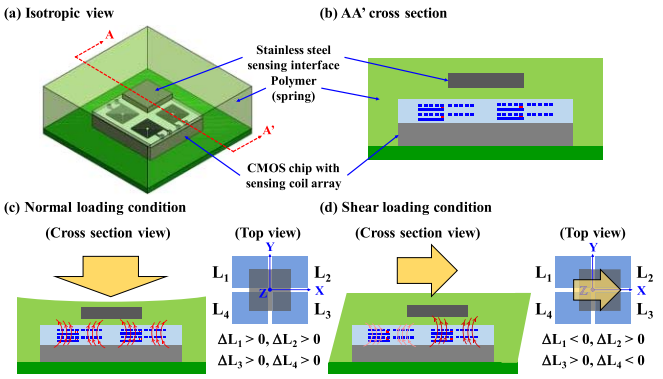

Fig. 1. Tri-axial inductive micro tactile sensor design concept, (a-b) structure schema including CMOS chip, stainless-steel sheet sensing interface, and polymer encapsulation, and (c-d) sensing principle for normal and shear loads.

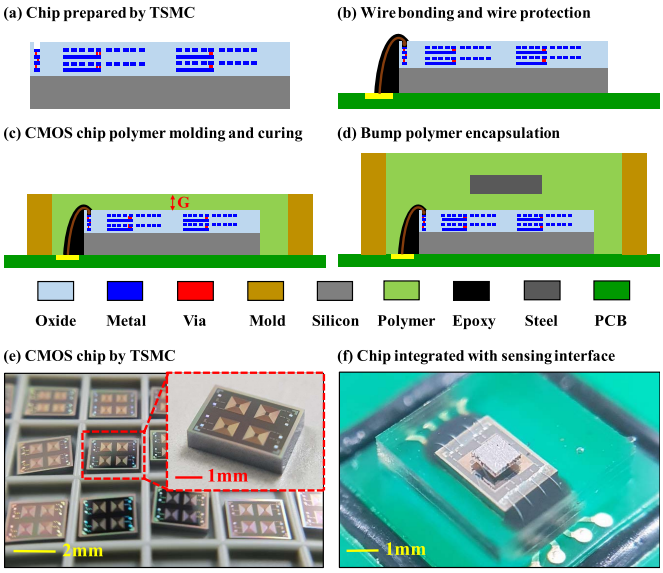

Fig. 2. (a-d) Fabrication and integration processes, and (e-f) typical results.

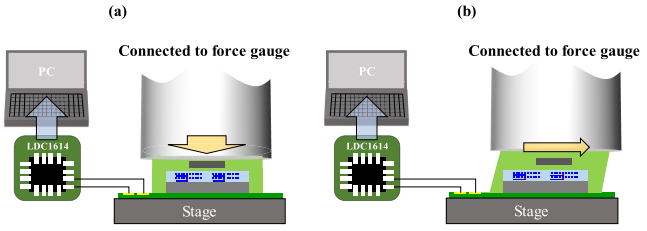

Fig. 3. The measurement setup for (a) normal, and (b) shear, load tests.

will reduce the gap between the CMOS chip and the stainless steel sheet (gap-closing effect) to increase the inductance signal of the sensing coils. As shown in Fig. 1d, the shear loads S_x and S_y (in the in-plane X- and Y-axes) will change the overlap region between the CMOS chip and the stainless steel sheet (area-change effect) to cause the inductance variation on each coil. In summary, the normal and shear loads will lead to the inductance change for each coil. Similar to the Wheatstone bridge signal calibration, the normal load-induced inductance change L_z, and the shear load-induced inductance changes L_x and L_y, can be extracted from the inductance changes ($L_1 \sim L_4$) measured from the 2×2 sensing coils [17]. The relation of extracted and measured inductance changes can be expressed as,

$$\begin{cases} L_x = L_2 + L_3 - L_1 - L_4 \\ L_y = L_1 + L_2 - L_3 - L_4 \\ L_z = L_1 + L_2 + L_3 + L_4 \end{cases} \quad (1)$$

As a result, the normal and shear loads can be detected by the proposed tri-axial tactile sensors with the 2×2 coil array on the CMOS chip.

III. Experiments and Results

Fig. 2 presents the implementation of the device. As shown in Fig. 2a, the CMOS chip was fabricated using the standard TSMC 0.35 μm 2P4M process. As depicted in Fig. 2b-c, after wire-bonding on PCB, the CMOS chip utilized the 1st polymer (SYLGARD PDMS184, Dow Corning, USA, with prepolymer:curing agent = 10:1) molding to define the gap G for polymer spring stiffness. As indicated in Fig. 2d, after the curing of 1st stage polymer at 120°C for 30 minutes, the stainless steel sheet was integrated and encapsulated with the CMOS chip using the 2nd polymer molding. Note that the stainless steel sheet (300 μm $\pm$ 3 μm in thickness) had its in-plane dimensions (1000 μm $\pm$ 5 μm in square) defined by a high-speed laser cutting system (LPKF StencilLaser G6080, LPKF Laser & Electronics AG, Germany, with a maximum energy of 150 W), and the stainless steel sheet is pick-placed using vacuum suction and a positioning stage. Fig. 2e displays CMOS chips fabricated by TSMC, and the 2×2 sensing coils are observed. Fig. 2f shows the CMOS chip (wire-bonded on PCB) and stainless steel sheet encapsulated by a polymer, which is the final device for testing.

Fig. 3a-b illustrates the measurement setups, respectively, for normal and shear loading tests. The load is applied to the device through a probe. The magnitude of the load is specified by the positioning stage and monitored by a commercial force gauge (FSH-50N, YOTEC Precision Instrument, Taiwan, 0.01 N resolution with maximum loading of 50 N). The inductance outputs of the sensing chip (4 channels) are rendered by using the commercially available circuit (LDC1614, Texas Instruments, USA, inductance to digital converter chip). The sensing scheme of LDC1614 is based on the resonant frequency drift of the LC tank [19]. Moreover, the readout circuit utilizes a reference frequency to detect the frequency of the LC tank. To meet the specifications of LDC1614 (within the frequency range of 1 kHz to 10 MHz), the additional inductor Ls (with a value of 22 μH) and the capacitor Cp (with a value of 30 pF) are required for the sensing coils, as depicted in Fig. 4a. Fig. 4b further shows the equivalent circuit model of the sensing scheme (for one channel), which includes the resistance (Rs) and parasitic capacitance ($C_{parasitic}$). Since the $C_{parasitic}$ is on the order of several hundred femto-Farads (nearly 2 orders of magnitude smaller than Cp), the effect of parasitic capacitance is ignored. As a result, the tactile load

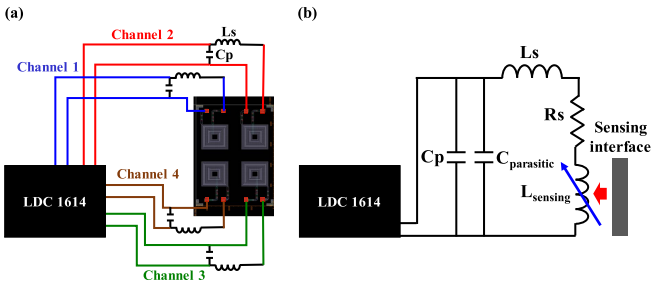

Fig. 4. The sensing scheme of the presented sensor by converting the inductance output using the commercially available chip LDC1614, (a) the electrical connection of the fabricated CMOS sensing chip and the LDC1614, and (b) the equivalent circuit for one channel.

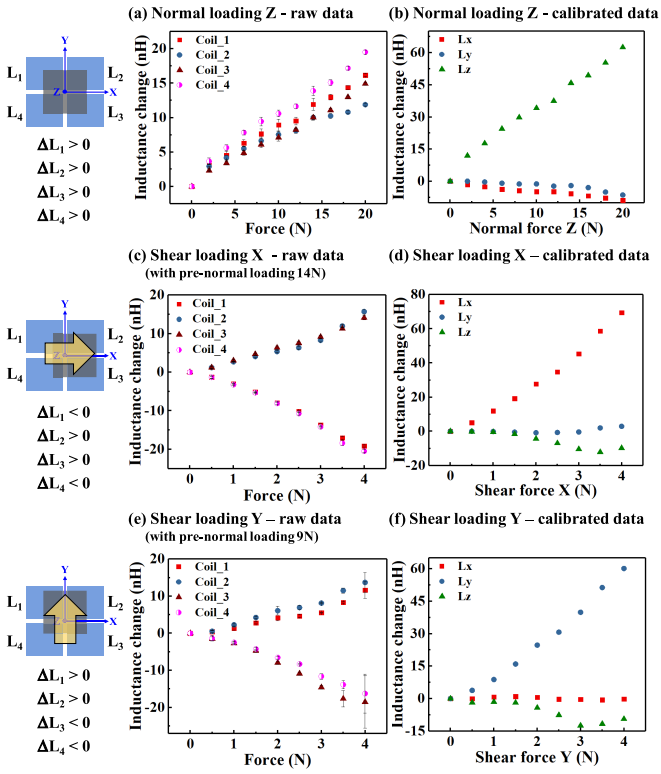

Fig. 5. The measurement results for (a-b) normal force (N_Z) response, (c-d) shear force (S_X) response, and (e-f) shear force (S_Y) response.

will lead to the change of magnetic field from coils and further cause the variation in inductance from the sensing chip; the inductance change is then detected by the frequency shift of the LDC1614.

Measurements in Fig. 5 present the typical force calibration results of the tri-axial tactile sensor. Measurement results in Fig. 5a show the inductance changes of four sensing coils under different normal loads (N_z). The normal tactile load reduced the gap between the stainless steel sheet and sensing coils; hence, the inductance on each coil was increased. Fig. 5b further shows the inductance change results extracted from Eq. (1). Fig. 5b indicates that the inductance change L_z is the dominant signal when under the normal tactile load N_z. Measurement results in Fig. 5c depict the inductance changes of four sensing coils under different X-axis shear loads (S_x). The shear load increased the overlap area between the stainless steel sheet and coils_2 ~ 3; hence, the inductance values on coils_2 ~ 3 were increased. On the other hand, the inductance values on coil_1 and coil_4 were decreased. Fig. 5d further shows the inductance change results extracted from Eq. (1) and indicates that the inductance change L_x is the dominant signal when under the shear load S_x. Similarly, the results in Fig. 5e-f, respectively, show the measured and extracted inductance changes for the Y-axis shear loads (S_y), and the inductance change L_y is the dominant signal. According to the typical measurement results, the presented tri-axial inductive tactile sensor exhibits the normal load (Z-axis) sensitivity of 2.9 nH/N, X-axis shear force sensitivity of 17.4 nH/N, and Y-axis shear force sensitivity of 15.3 nH/N. Note that any lateral misalignment of the stainless steel sheet with the underlying sensing coils during the integration process (Fig. 2d), and any variation in the sensing gap flatness defined in Fig. 2c, may cause the drift of the sensing signal for each coil. For example, the variation in inductance change with force for each sensing coil is slightly different in Fig. 5a. The sensing signal offset can be improved with further process optimization and the commercial pick-place equipment (with alignment accuracy ranging from ± 2.5 μm to ± 50 μm). In summary, the proposed CMOS-MEMS inductive tri-axial tactile sensor design performance has been demonstrated by the experimental results.

IV. Conclusion

This study presents a simple inductive tri-axial tactile sensor by using the polymer encapsulation/integration of a CMOS chip with a sensing coil array and a stainless steel sheet sensing interface. The devices are implemented by using the commercially available standard CMOS chip process (offered by TSMC) and stainless steel laser-cut machining. No fragile suspended thin film mechanical components are required for the presented devices. The normal load (N_z) is detected by the inductance change resulting from the variation of the sensing gap, while the in-plane shear loads (S_x, S_y) are detected by the inductance change resulting from the variation of the sensing area on the coil array. The measurements indicate that the presented sensor could distinguish tactile loads in different directions, and its sensitivities are 2.9 nH/N for the normal load (Z-axis), 17.4 nH/N for the shear load along the X-axis, and 15.3 nH/N for the shear load along the Y-axis.

References

[1] *Small 3-Axis Force Sensor*, Tec Gihan Co., Ltd, Kyoto, Japan, 2006.
[2] D. V. Dao and S. Sugiyama, "Fabrication and characterization of 4-DOF soft-contact tactile sensor and application to robot fingers," in *Proc. IEEE Int. Symp. Micro Nano Mech. Hum. Sci.*, Nov. 2006, pp. 1–6. doi: 10.1109/MHS.2006.320271.
[3] J.-H. Kim, W.-C. Choi, H.-J. Kwon, and D.-I. Kang, "Development of tactile sensor with functions of contact force and thermal sensing for attachment to intelligent robot finger tip," *IEEE Sensors*, Oct. 2006, pp. 1468–1472. doi: 10.1109/ICSENS.2007.355911.
[4] G. Vásárhelyi, M. Ádám, É. Vázsonyi, Z. Vízváry, A. Kis, I. Bársony, and C. Dücsõ, "Characterization of an integrable single-crystalline 3-D tactile sensor," *IEEE Sensors J.*, vol. 6, no. 4, pp. 928–934, Aug. 2006. doi: 10.1109/JSEN.2006.877990.
[5] A. Sieber, P. Valdastri, K. Houston, A. Menciassi, and P. Dario, "Flip chip microassembly of a silicon triaxial force sensor on flexible substrates," *Sens. Actuators A, Phys.*, vol. 142, no. 1, pp. 421–428, 2008. doi: 10.1016/j.sna.2007.02.042.

[6] C.-C. Wen and W. Fang, "Tuning the sensing range and sensitivity of three axes tactile sensors using the polymer composite membrane," *Sens. Actuators A, Phys.*, vols. 145–146, pp. 14–22, Jul./Aug. 2008. doi: 10.1016/j.sna.2007.10.011.

[7] H. Takahashi, A. Nakaia, N. Thanh-Vinh, K. Matsumoto, and I. Shimoyama, "A triaxial tactile sensor without crosstalk using pairs of piezoresistive beams with sidewall doping," *Sens. Actuators A, Phys.*, vol. 199, pp. 43–48, Sep. 2013. doi: 10.1016/j.sna.2013.05.002.

[8] N. Thanh-Vinh, N. Binh-Khiem, H. Takahashi, K. Matsumoto, and I. Shimoyama, "High-sensitivity triaxial tactile sensor with elastic microstructures pressing on piezoresistive cantilevers," *Sens. Actuators A, Phys.*, vol. 215, pp. 167–175, Aug. 2014. doi: 10.1016/j.sna.2013.09.002.

[9] M. Hosono, K. Noda, K. Matsumoto, and I. Shimoyama, "Dynamic performance analysis of a micro cantilever embedded in elastomer," *J. Micromech. Microeng.*, vol. 25, no. 7, 2014, Art. no. 075006. doi: 10.1088/0960-1317/25/7/075006.

[10] R. A. Brookhuis, R. J. Wiegerink, T. S. J. Lammerink, M. J. de Boer, K. Ma, and M. C. Elwenspoek, "Scalable six-axis force-torque sensor with a large range for biomechanical applications," in *Proc. IEEE MEMS*, Jan./Feb. 2012, pp. 595–598. doi: 10.1109/MEMSYS.2012.6170258.

[11] R. A. Brookhuis, R. J. Wiegerink, T. S. J. Lammerink, K. Ma, and G. J. M. Krijnen, "Large range multi-axis fingertip force sensor," in *Proc. 17th Int. Conf. Solid-State Sensors, Actuat. Microsyst.*, Jun. 2013, pp. 2737–2740. doi: 10.1109/Transducers.2013.6627372.

[12] D. Alveringh, R. A. Brookhuis, R. J. Wiegerink, and G. J. M. Krijnen, "A large range multi-axis capacitive force/torque sensor realized in a single SOI wafer," in *Proc. IEEE MEMS*, Jan. 2014, pp. 680–683. doi: 10.1109/MEMSYS.2014.6765732.

[13] M. Makihata, S. Tanaka, M. Muroyama, S. Matsuzaki, H. Yamada, T. Nakayama, U. Yamaguchi, K. Mima, Y. Nonomura, M. Fujiyoshi, and M. Esashi, "Integration and packaging technology of MEMS-on-CMOS capacitive tactile sensor for robot application using thick BCB isolation layer and backside-grooved electrical connection," *Sens. Actuators A, Phys.*, vol. 188, pp. 103–110, Dec. 2012. doi: 10.1016/j.sna.2012.04.032.

[14] S. Asano, M. Muroyama, T. Bartley, T. Nakayama, U. Yamaguchi, H. Yamada, Y. Hata, Y. Nonomura, and S. Tanaka, "3-Axis fully-integrated surface-mountable differential capacitive tactile sensor by CMOS flip-bonding," in *Proc. IEEE MEMS*, Jan. 2016, pp. 850–853. doi: 10.1109/MEMSYS.2016.7421763.

[15] Y. Hata, Y. Suzuki, M. Muroyama, T. Nakayama, Y. Nonomura, R. Chand, H. Hirano, Y. Omura, M. Fujiyoshi, and S. Tanaka, "Integrated 3-axis tactile sensor using quad-seesaw-electrode structure on platform LSI with through silicon vias," *Sens. Actuators A, Phys.*, vol. 273, pp. 30–41, Apr. 2018. doi: 10.1016/j.sna.2018.02.013.

[16] S. Wattanasarn, K. Noda, K. Matsumoto, and I. Shimoyama, "3D flexible tactile sensor using electromagnetic induction coils," in *Proc. IEEE MEMS*, Jan./Feb. 2012, pp. 488–491. doi: 10.1109/MEMSYS.2012.6170230.

[17] H. Wang, D. Jones, G. de Boer, J. Kow, L. Beccai, A. Alazmani, and P. Culmer, "Design and characterization of tri-axis soft inductive tactile sensors," *IEEE Sensors J.*, vol. 18, no. 19, pp. 7793–7801, Oct. 2018. doi: 10.1109/JSEN.2018.2845131.

[18] S.-K. Yeh, H.-C. Chang, and W. Fang, "Development of CMOS MEMS inductive type tactile sensor with the integration of chrome steel ball force interface," *J. Micromech. Microeng.*, vol. 28, no. 4, 2018, Art. no. 044005. doi: 10.1088/1361-6439/aaac24.

[19] *Inductance to digital converter LDC1614*. Accessed: Mar. 25, 2018. [Online]. Available: http://www.ti.com/product/LDC1614